

Hydrodynamics and global structure of rotating Schwarzschild black holes

Soon-Tae Hong*

Department of Science Education, Ewha Womans University, Seoul 120-750 Korea

Sung-Won Kim†

*Department of Science Education, Ewha Womans University, Seoul 120-750 Korea and
Asia Pacific Center for Theoretical Physics, Pohang 790-784 Korea*

(Dated: November 7, 2018)

Exploiting a rotating Schwarzschild black hole metric, we study hydrodynamic properties of perfect fluid whirling inward toward the black holes along a conical surface. On the equatorial plane of the rotating Schwarzschild black hole, we derive radial equations of motion with effective potentials and the Euler equation for steady state axisymmetric fluid. Moreover, numerical analysis is performed to figure out effective potentials of particles on the rotating Schwarzschild manifolds in terms of angular velocity, total energy and angular momentum per unit rest mass. Higher dimensional global embeddings are also constructed inside and outside the event horizons of the rotating Schwarzschild black holes.

PACS numbers: 02.40.Ma, 04.20.Dw, 04.20.Jb, 04.70, 95.30.L

Keywords: rotating Schwarzschild black hole, hydrodynamics, Euler equation, global flat embedding

I. INTRODUCTION

The physics of a rotating charged sphere has long attracted the attention of physicists [1, 2, 3]. From the experimental viewpoint, the pulsars have given concrete evidence for the existence of rotating magnetized collapsed objects. From the theoretical viewpoint, the existing exact solutions of Einstein equations have shown that the most general stationary solution, which is asymptotically flat with a regular horizon for a fully collapsed object, has to be rotating and endowed with a net charge. It is well known that the Kerr [4] family of solutions of the Einstein and Einstein-Maxwell equations is the general class of solutions which could represent the field of a rotating neutral or electrically charged sphere in asymptotically flat space. In the extended manifolds, all geodesics which do not reach the central ring singularities of the Kerr black hole are shown to be complete, and also those null or timelike geodesics which do reach the singularities are entirely confined to the equator [5]. Moreover, the Kerr metric has the region called the ergosphere where the asymptotic time translation Killing field becomes spacelike. In the ergosphere, all observers are forced to rotate in the direction of the rotation of the black hole. Recently, the rotating Schwarzschild wormhole metric was proposed to investigate classes of geodesics falling through it which do not encounter any energy condition violating matter [6].

On the other hand, a familiar feature of exact solutions to the field equations of general relativity is the presence of singularities. As novel ways of removing the coordinate singularities, the higher dimensional global flat em-

beddings of the black hole solutions are subjects of great interest both to mathematicians and to physicists. In differential geometry, it has been well-known that four dimensional Schwarzschild metric [7] is not embedded in R^5 [8]. Recently, (5+1) dimensional global embedding Minkowski space (GEMS) structure for the Schwarzschild black hole has been obtained [9] to investigate a thermal Hawking effect on a curved manifold [10] associated with an Unruh effect [11] in these higher dimensional spacetime. In (3+1) dimensions, the global flat embeddings inside and outside of event horizons of Schwarzschild and Reissner-Nordström black holes, have been constructed and on these overall patches of the curved manifolds four accelerations and Hawking temperatures have been evaluated by introducing relevant Killing vectors [12]. Recently, the GEMS scheme has been applied to stationary motions in spherically symmetric spacetime [13], and the Banados-Teitelboim-Zanelli black hole [14] has been embedded in (3+2) dimensions to investigate the $SO(3,2)$ global and $Sp(2)$ local symmetries [15].

In this paper, we take an ansatz for a rotating Schwarzschild black hole to investigate hydrodynamic properties of the perfect fluid spiraling inward toward the black holes along a conical surface. On the rotating Schwarzschild black hole manifolds we then construct higher dimensional global embeddings inside and outside the event horizons of the black holes. We also perform numerical evaluations of effective potentials of particles on the equatorial planes of the rotating Schwarzschild black holes in terms of angular velocity, total energy and angular momentum per unit rest mass.

This paper is organized as follows. In section II we study the rotating Schwarzschild black hole with constant angular velocity, and in section III we investigate that with angular velocity proportional to $1/r^3$. Section IV includes summary and discussions.

*Electronic address: soonhong@ewha.ac.kr

†Electronic address: sungwon@ewha.ac.kr

II. ROTATING SCHWARZSCHILD BLACK HOLE WITH CONSTANT Ω

We consider the rotating Schwarzschild black hole with a constant angular velocity Ω whose 4-metric is described as

$$ds^2 = -N^2 dt^2 + N^{-2} dr^2 + r^2 d\theta^2 + r^2 \sin^2 \theta (d\phi - \Omega dt)^2. \quad (2.1)$$

Here in the units $G = c = 1$ the lapse function N^2 is defined as

$$N^2 = 1 - \frac{2m}{r} = \frac{r - r_H}{r}. \quad (2.2)$$

The event horizon r_H is located at the pole of g_{rr} , namely at the root of N^2 to yield $r_H = 2m$ as in the static Schwarzschild black hole case. The four velocity is given by

$$u^a = \frac{dx^a}{d\tau}, \quad (2.3)$$

where we can choose τ to be the proper time (affine parameter) for timelike (null) geodesics. From the equation of motion of a test particle in the rotating Schwarzschild manifold, the particle initially at rest at infinity spiral inward toward the black hole along a conical surface of constant $\theta = \theta_\infty$ where θ_∞ is the polar angle at infinity. For a fluid which is at rest at infinity and approaches supersonically to the black hole, one may take the approximation to simplify the hydrodynamical equations

$$u^\theta = \frac{d\theta}{d\tau} \approx 0. \quad (2.4)$$

As in the Schwarzschild black hole since the coordinates t and ϕ are cyclic we have the timelike Killing field ξ^a and the axial Killing field ψ^a . Corresponding to the Killing fields ξ^a and ψ^a we can then find the conserved energy E and the angular momentum L per unit rest mass for geodesics given as follows

$$\begin{aligned} E &= -g_{ab}\xi^a u^b \\ &= \left(\frac{r - r_H}{r} - \Omega^2 r^2 \sin^2 \theta \right) u^t + \Omega r^2 \sin^2 \theta u^\phi, \\ L &= g_{ab}\psi^a u^b = -\Omega r^2 \sin^2 \theta u^t + r^2 \sin^2 \theta u^\phi, \end{aligned} \quad (2.5)$$

where u^a are four velocity of the locally nonrotating observers defined by (2.3). Moreover, we can introduce a new conserved parameter κ defined as

$$\kappa = -g_{ab}u^a u^b \quad (2.6)$$

whose values are given by $\kappa = 1$ for timelike geodesics and $\kappa = 0$ for null geodesics.

In the case of geodesics on the equatorial plane $\phi = \pi/2$, u^t and u^ϕ are given in terms of E and L as follows

$$\begin{aligned} u^t &= \frac{r}{r - r_H} E - \frac{\Omega r}{r - r_H} L \\ u^\phi &= \frac{\Omega r}{r - r_H} E + \left(\frac{1}{r^2} - \frac{\Omega^2 r}{r - r_H} \right) L, \end{aligned} \quad (2.7)$$

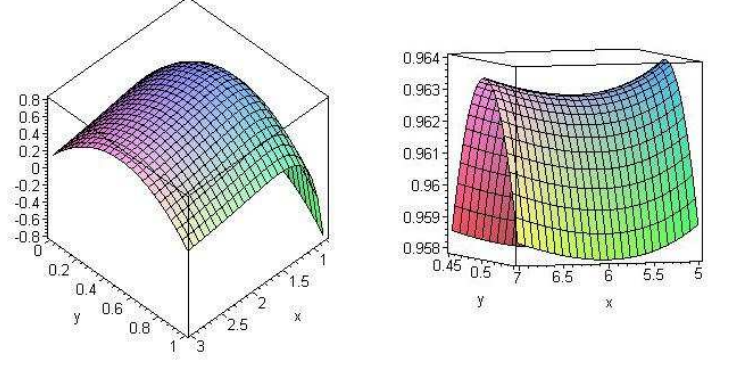


FIG. 1: Effective potentials $V(x, y)$ with $x = r/r_H$ and $y = \Omega r_H$ for null and timelike geodesics of particles with $E = 1$ and $L = 2r_H$.

which are substituted into (2.6) to yield the radial equation for the particle on the equatorial plane

$$\frac{1}{2}E^2 = \frac{1}{2}u^r u^r + V(r, E, L), \quad (2.8)$$

with the effective potential

$$V = -\frac{r_H}{2r}\kappa + \frac{L^2}{2r^2} + \frac{1}{2}\kappa - \frac{L}{r^3} \left[\left(\frac{r_H}{2} + \frac{\Omega^2 r^3}{2} \right) L - \Omega r^3 E \right]. \quad (2.9)$$

Here the first and second terms denote the Newtonian and centrifugal barrier terms respectively, which are attainable from Newtonian mechanics, while the other terms are general relativistic corrections, including the black hole rotating effects with the parameter Ω . If $E < 1$ the orbit of the particle is bound so that it cannot reach infinity, while if $E > 1$ the orbit is unbound except for a measure-zero set of unstable orbits [16].

For the null geodesics with $\kappa = 0$, we find the only extremum of the effective potential to be a maximum occurring at $r = 3r_H/2$ as in the case of static Schwarzschild black hole. The effective potential $V(x, y)$ for the particles with the total energy per unit rest mass $E = 1$ and angular momentum per unit rest mass $L = 2r_H$ is shown in the left graph in Fig. 1 where x and y denote the dimensionless variables $x = r/r_H$ and $y = \Omega r_H$, respectively. Here note that we have a maximal effective potential at the position $(x, y) = (3/2, 1/2)$.

Next, we consider the timelike geodesics. The effective potential (2.9) with $\kappa = 1$ now should fulfil the condition

$$\frac{dV}{dr} = 0, \quad (2.10)$$

to yield the radii of the stable and unstable bound orbits on the equatorial plane for $L^2 > 3r_H^2$

$$r_{s,us} = \frac{L^2 \pm L(L^2 - 3r_H^2)^{1/2}}{r_H} \quad (2.11)$$

where the upper (lower) sign refers to the stable (unstable) orbit. In particular, for the case of $L \gg r_H$, we can

find $r_s \approx 2L^2/r_H$ corresponding to the Newtonian radius of circular orbits of particles with angular momentum per mass L orbiting a spherical body of mass m . The energy per unit mass of the particle in the circular orbit of the radius $r = r_s$ is the value of the effective potential V at that radius

$$\frac{1}{2}E^2 = V(r), \quad (2.12)$$

which yields, together with (2.10), the energy per unit mass

$$E_s = \frac{2^{1/2}(r_s - r_H)}{r_s^{1/2}(2r_s - 3r_H)^{1/2}} + \frac{\Omega r_H^{1/2} r_s}{(2r_s - 3r_H)^{1/2}}. \quad (2.13)$$

Note that we have an term proportional to Ω additional to the static Schwarzschild black hole result. If a particle is displaced slightly from the equilibrium radius r_s of the stable circular orbit, the particle will oscillate in the radius about r_s to execute simple harmonic motion with frequency ω_r given by

$$\omega_r = \frac{r_H^{1/2}(r_s - 3r_H)^{1/2}}{r_s^{3/2}(2r_s - 3r_H)^{1/2}}. \quad (2.14)$$

On the other hand, the angular frequency ω_ϕ for the circular orbit is found to be

$$\omega_\phi = \frac{r_H^{1/2} + 2^{1/2}\Omega r_s^{3/2}}{r_s(2r_s - 3r_H)^{1/2}}. \quad (2.15)$$

Here note that the frequency ω_r is the same as that in the static Schwarzschild black hole case, while the angular frequency ω_ϕ is enhanced by the additional term proportional to Ω . For the timelike geodesics of the particles with the total energy per unit rest mass $E = 1$ and angular momentum per unit rest mass $L = 2r_H$, the effective potential $V(x, y)$ has a shape similar to that for the null geodesic case shown in Fig. 1. However, along the curve $y = 1/2$ we have maximal potential values to yield a maximal effective potential at the position $(x, y) = (2, 1/2)$ and a saddle point of the effective potential at the position $(x, y) = (6, 1/2)$ as shown in the right graph in Fig. 1.

Now, we consider the global aspects of the rotating Schwarzschild black hole. After some algebra, for the rotating Schwarzschild black hole in the region $r \geq r_H$ we can obtain the (5+1) GEMS structure

$$ds^2 = -(dz^0)^2 + (dz^1)^2 + (dz^2)^2 + (dz^3)^2 + (dz^4)^2 + (dz^5)^2 \quad (2.16)$$

with the coordinate transformations

$$\begin{aligned} z^0 &= k_H^{-1} \left(\frac{r - r_H}{r} \right)^{1/2} \sinh k_H t, \\ z^1 &= k_H^{-1} \left(\frac{r - r_H}{r} \right)^{1/2} \cosh k_H t, \\ z^2 &= r \sin \theta \cos(\phi - \Omega t), \end{aligned}$$

$$\begin{aligned} z^3 &= r \sin \theta \sin(\phi - \Omega t), \\ z^4 &= r \cos \theta, \\ z^5 &= \int dr \left(\frac{r_H(r^2 + r_H r + r_H^2)}{r^3} \right)^{1/2} \equiv f(r, r_H), \end{aligned} \quad (2.17)$$

where the surface gravity k_H is given by

$$k_H = \frac{1}{2r_H}. \quad (2.18)$$

Here we recall that the static Schwarzschild is embedded in (5+1) dimensions with the GEMS structure (2.16) and the coordinate transformations for $r \geq r_H$ [9]

$$\begin{aligned} z^0 &= k_H^{-1} \left(\frac{r - r_H}{r} \right)^{1/2} \sinh k_H t, \\ z^1 &= k_H^{-1} \left(\frac{r - r_H}{r} \right)^{1/2} \cosh k_H t, \\ z^2 &= r \sin \theta \cos \phi, \\ z^3 &= r \sin \theta \sin \phi, \\ z^4 &= r \cos \theta \\ z^5 &= f(r), \end{aligned} \quad (2.19)$$

where $f(r)$ is read off from (2.17). Here one can readily check that in the limit $\Omega \rightarrow 0$ the embedding (2.17) reduces to that of the Schwarzschild case (2.19). In order to investigate the region $r \leq r_H$ we rewrite the rotating Schwarzschild black hole four-metric (2.1) as

$$ds^2 = \bar{N}^2 dt^2 - \bar{N}^{-2} dr^2 + r^2 d\theta^2 + r^2 \sin^2 \theta (d\phi - \Omega dt)^2, \quad (2.20)$$

in terms of the positive definite lapse function inside the event horizon r_H

$$\bar{N}^2 = -1 + \frac{2M}{r} = \frac{r_H - r}{r} \quad (2.21)$$

to yield the (5+1) GEMS structure (2.16) with the coordinate transformation

$$\begin{aligned} z^0 &= k_H^{-1} \left(\frac{r_H - r}{r} \right)^{1/2} \cosh k_H t, \\ z^1 &= k_H^{-1} \left(\frac{r_H - r}{r} \right)^{1/2} \sinh k_H t, \\ z^5 &= f(r), \end{aligned} \quad (2.22)$$

with (z^2, z^3, z^4) in (2.17).

III. ROTATING SCHWARZSCHILD BLACK HOLE WITH $\Omega = 2a/r^3$

Now, we consider the rotating Schwarzschild black hole with the angular velocity of the form $\Omega = 2a/r^3$ [6] by

introducing 4-metric

$$ds^2 = -N^2 dt^2 + N^{-2} dr^2 + r^2 d\theta^2 + r^2 \sin^2 \theta \left(d\phi - \frac{2a}{r^3} dt \right)^2, \quad (3.1)$$

where a is the angular momentum of the black hole. As in the rotating Schwarzschild black hole case with constant Ω in the previous section, we have the timelike Killing field ξ^a and the axial Killing field ψ^a to yield the conserved energy E and the angular momentum L per unit rest mass for geodesics

$$\begin{aligned} E &= \left(\frac{r - r_H}{r} - \frac{4a^2 \sin^2 \theta}{r^4} \right) u^t + \frac{2a \sin^2 \theta}{r} u^\phi, \\ L &= -\frac{2a \sin^2 \theta}{r} u^t + r^2 \sin^2 \theta u^\phi. \end{aligned} \quad (3.2)$$

On the equatorial plane, we can readily express u^t and u^ϕ in terms of E and L as in (2.7) to yield the radial equation for the particle on the equatorial plane (2.8) with the effective potential

$$V = -\frac{r_H}{2r} \kappa + \frac{L^2}{2r^2} + \frac{1}{2} \kappa - \frac{L}{r^3} \left[\left(\frac{r_H}{2} + \frac{2a^2}{r^3} \right) L - 2aE \right]. \quad (3.3)$$

Here note that the last terms associated with $-L/r^3$ dominate over the centrifugal barrier term at small r . In the vanishing a limit (or equally in the $\Omega = 0$ case in (2.1)), we can easily see that the effective potential V in (3.3) reduces to the Schwarzschild black hole case.

For the null geodesics with $\kappa = 0$, we find the only maximum of the effective potential occurring at

$$r \geq \frac{3}{2} r_H - \frac{6aE}{L}. \quad (3.4)$$

The effective potentials $V(x, y)$ for the null geodesics of the particles with the total energy per unit rest mass $E = 1$ and angular momentum per unit rest mass $L = 2r_H$ are shown in the left graph in Fig. 2. Here x and y represent the dimensionless variables $x = r/r_H$ and $y = a/r_H^2$. Here observe that along the $y = x^3/4$ curve we have maximal potential values to yield maximal effective potential values.

For the timelike geodesics with the effective potential (3.3) with $\kappa = 1$, the condition (2.10) yields the radius r_s of the stable bound orbits which satisfy on the equatorial plane

$$r_H r_s^5 - 2L^2 r_s^4 + 3(L^2 r_H - 4aLE) r_s^3 + 24a^2 L^2 = 0. \quad (3.5)$$

The energy per unit mass of the particle in the circular orbit of the radius $r = r_s$ is found to have the energy lower bound for $r_s^4 \geq 12a^2$

$$E_s \geq \left(1 - \frac{r_H}{r_s} + \frac{r_H(r_s^4 - r_H r_s^3 - 4a^2)}{r_s(2r_s^4 - 2r_H r_s^3 - 24a^2)} \right)^{1/2}. \quad (3.6)$$

The effective potentials $V(x, y)$ for the null and timelike geodesics of the particles with the total energy per unit

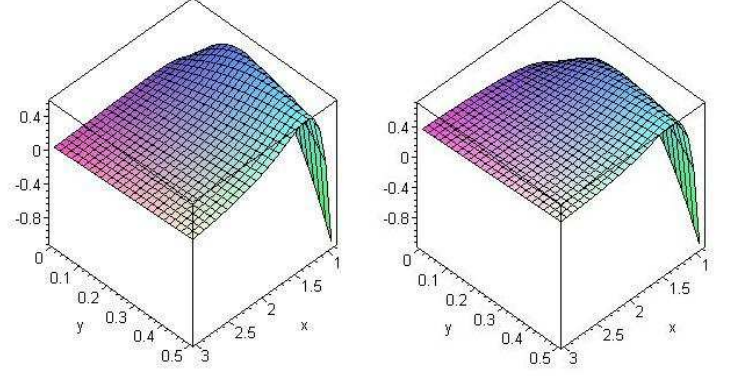


FIG. 2: Effective potentials $V(x, y)$ with $x = r/r_H$ and $y = a/r_H^2$ for null and timelike geodesics of particles with $E = 1$ and $L = 2r_H$.

rest mass $E = 1$ and angular momentum per unit rest mass $L = 2r_H$ are shown in the right graph in Fig. 2 with x and y being the dimensionless variables $x = r/r_H$ and $y = a/r_H^2$. As in the null geodesic case, along the $y = x^3/4$ curve we have maximal potential values to yield maximal effective potential values.

The fundamental equations of relativistic fluid dynamics can be obtained from the conservation of particle number and energy-momentum fluxes. In order to derive an equation for the conservation of particle numbers one can use the particle flux four vector nu^a [17]

$$\nabla_a(nu^a) = \frac{1}{\sqrt{-g}} \nabla_a(\sqrt{-g} nu^a) = 0, \quad (3.7)$$

where n is the proper number density of particles measured in the rest frame of the fluid and ∇_a is the covariant derivative in the rotating Schwarzschild curved manifold and $g = \det g_{ab}$. For steady state axisymmetric flow, the conservation of energy-momentum fluxes is similarly described by the Einstein equation [18]

$$\nabla_b T_a^b = \frac{1}{\sqrt{-g}} \nabla_b(\sqrt{-g} T_a^b) = 0, \quad (3.8)$$

where the stress-energy tensor T^{ab} for perfect fluid is given by

$$T^{ab} = \rho u^a u^b + (g^{ab} + u^a u^b) P \quad (3.9)$$

with ρ and P being the proper internal energy density, including the rest mass energy, and the isotropic gas pressure, respectively. The Einstein equation (3.8) can be rewritten in another covariant form

$$u_a \nabla_b((P + \rho)u^b) + (P + \rho)u^b \nabla_b u_a + \nabla_a P = 0. \quad (3.10)$$

Multiplying (3.10) by u^a we can project it on the direction of the four velocity to obtain

$$nu^a \left(\nabla_a \left(\frac{P + \rho}{n} \right) - \frac{1}{n} \nabla_a P \right) = 0, \quad (3.11)$$

where the continuity equation (3.7) has been used. The radial component of (3.11) yields

$$\frac{d\rho}{dr} - \frac{P + \rho}{n} \frac{dn}{dr} = \frac{\Lambda - \Gamma}{u^r}. \quad (3.12)$$

Here the energy loss Λ and the energy gain Γ are introduced to set the decrease in the entropy of inflowing gas equal to the difference $\Lambda - \Gamma$. Moreover, using the projection operator $g_{ab} + u_a u_b$ in the equation (3.10) we can obtain the general relativistic Euler equation on the direction perpendicular to the four velocity

$$(P + \rho)u^b \nabla_b u_a + (g_{ab} + u_a u_b) \nabla^b P = 0. \quad (3.13)$$

After some algebra, from (3.13) we obtain the radial com-

ponent of the Euler equation for the steady state axisymmetric fluid

$$\frac{d}{dr}(u^r u^r) + \frac{r_H}{r^2} + \frac{2}{P + \rho} \left(u^r u^r + 1 - \frac{r_H}{r} \right) \frac{dP}{dr} = 0. \quad (3.14)$$

Here it is interesting to see that the results (3.12) and (3.14) hold also in the rotating Schwarzschild black hole with the constant Ω and even in the static Schwarzschild black hole.

Next, we consider the global embeddings of the rotating Schwarzschild manifold with the angular velocity $\Omega = 2a/r^3$. After tedious algebra, for the rotating Schwarzschild black hole in the region $r \geq r_H$ we can obtain the (8+6) GEMS structure

$$ds^2 = -(dz^0)^2 + (dz^1)^2 + (dz^2)^2 + (dz^3)^2 + (dz^4)^2 - (dz^5)^2 - (dz^6)^2 - (dz^7)^2 + (dz^8)^2 + (dz^9)^2 + (dz^{10})^2 - (dz^{11})^2 - (dz^{12})^2 + (dz^{13})^2 \quad (3.15)$$

with the coordinate transformations

$$\begin{aligned} z^0 &= k_H^{-1} \left(\frac{r - r_H}{r} \right)^{1/2} \sinh k_H t, \\ z^1 &= k_H^{-1} \left(\frac{r - r_H}{r} \right)^{1/2} \cosh k_H t, \\ z^2 &= \left(\frac{r^3 + 2a}{r} \right)^{1/2} \sin \theta \cos \phi, \\ z^3 &= \left(\frac{r^3 + 2a}{r} \right)^{1/2} \sin \theta \sin \phi, \\ z^4 &= \left(\frac{r^3 + 2a}{r} \right)^{1/2} \cos \theta, \\ z^5 &= \left(\frac{2a}{r} \right)^{1/2} \sin \theta \cos(\phi + t), \\ z^6 &= \left(\frac{2a}{r} \right)^{1/2} \sin \theta \sin(\phi + t), \\ z^7 &= \left(\frac{2a}{r} \right)^{1/2} \cos \theta, \\ z^8 &= \left(\frac{2a(r^3 + 2a)}{r^4} \right)^{1/2} \sin \theta \cos t, \\ z^9 &= \left(\frac{2a(r^3 + 2a)}{r^4} \right)^{1/2} \sin \theta \sin t, \\ z^{10} &= \left(\frac{4a(r^3 + 2a)}{r^4} \right)^{1/2} \cos \theta, \\ z^{11} &= \left(\frac{2a(r^3 + 2a)}{r^4} \right)^{1/2} \sin \theta, \end{aligned}$$

$$\begin{aligned} z^{12} &= \left(\frac{r^3 + 2a}{r} \right)^{1/2}, \\ z^{13} &= \int dr \left(\frac{2r_H(r^2 + rr_H + r_H^2) + 2r^3 + a}{2r^3} \right)^{1/2} \\ &\equiv g(r), \end{aligned} \quad (3.16)$$

where k_H is given by (2.18). Note that in the limit $a \rightarrow 0$ the embedding (3.16) reduces to the Schwarzschild case. In fact, $(z^0, z^1, z^2, z^3, z^4)$ go to those in the Schwarzschild black hole (2.19) and $(z^5, z^6, z^7, z^8, z^9, z^{10}, z^{11})$ disappear. Moreover, we find

$$\begin{aligned} -(dz^{12})^2 + (dz^{13})^2 &= \\ -\frac{(r^3 - a)^2}{r^3(r^3 + 2a)} dr^2 + \frac{2r_H(r^2 + rr_H + r_H^2) + 2r^3 + a}{2r^3} dr^2, \end{aligned} \quad (3.17)$$

which, in the vanishing a limit, becomes $(df)^2$ in (2.17) so that (z^{12}, z^{13}) merges into z^5 in the Schwarzschild black hole (2.19). When the black hole rotates sufficiently fast, g_{tt} becomes negative as in the Kerr black hole to yield the ergosphere where

$$r_H < r < 2a \sin \theta. \quad (3.18)$$

Here note that the above embedding (3.16) covers without any singularities the whole patch on $r > r_H$ inert to the presence of the ergosphere.

Next, in order to investigate the region $r \leq r_H$ we rewrite the rotating Schwarzschild black hole 4-metric (3.1) as

$$ds^2 = \bar{N}^2 dt^2 - \bar{N}^{-2} dr^2 + r^2 d\theta^2 + r^2 \sin^2 \theta \left(d\phi - \frac{2a}{r^3} dt \right)^2, \quad (3.19)$$

in terms of the positive definite lapse function (2.21) inside the event horizon r_H to yield the (8+6) GEMS structure (3.15) with the coordinate transformation

$$\begin{aligned} z^0 &= k_H^{-1} \left(\frac{r_H - r}{r} \right)^{1/2} \cosh k_H t, \\ z^1 &= k_H^{-1} \left(\frac{r_H - r}{r} \right)^{1/2} \sinh k_H t, \\ z^{13} &= g(r), \end{aligned} \quad (3.20)$$

with $(z^2, z^3, z^4, z^5, z^6, z^7, z^8, z^9, z^{10}, z^{11}, z^{12})$ in (3.16).

IV. CONCLUSIONS

In conclusion, taking an ansatz for a rotating Schwarzschild black hole analogous to the rotating Schwarzschild wormhole [6] we have investigated hydrodynamic properties of the perfect fluid spiraling inward toward the black holes along a conical surface. Here we have exploited the fact that the coordinates t and ϕ are

cyclic in the rotating Schwarzschild metric to find the timelike Killing field and the axial Killing field, to which we could obtain the conserved energy and the angular momentum per unit rest mass for geodesics.

On the equatorial plane of the rotating Schwarzschild black hole, we have derived the radial equations of motion with the effective potential. We have also performed numerical analysis of the effective potentials of particles on the rotating Schwarzschild manifolds in terms of angular velocity, total energy and angular momentum per unit rest mass. Finally, we have studied the rotating Schwarzschild black hole manifolds to construct (8+6) higher dimensional global embeddings inside and outside the event horizons.

Acknowledgments

We would like to acknowledge financial support in part from the Korea Science and Engineering Foundation Grant R01-2000-00015.

-
- [1] L.I. Schiff, Proc. Nat. Acad. Sci. **25**, 391 (1939).
 - [2] P.M.S. Blackett, Phil. Trans. Roy. Soc. Lon. **245**, 309 (1952).
 - [3] R. Ruffini and A. Treves, Astroph. Lett. **13**, 109 (1972).
 - [4] R.P. Kerr, Phys. Rev. Lett. **11**, 237 (1963).
 - [5] B. Carter, Phys. Rev. **174**, 1559 (1968).
 - [6] E. Teo, Phys. Rev. D **58**, 024014 (1998).
 - [7] K. Schwarzschild, Sitzber. Deut. Akad. Wiss. Berlin, KI. Math.-Phys. Tech. pp. 189-196 (1916).
 - [8] M. Spivak, *Differential Geometry* (Publish or Perish, Berkeley 1975) Vol 5, Chapter 11.
 - [9] S. Deser and O. Levin, Class. Quant. Grav. **14**, L163 (1997); S. Deser and O. Levin, Class. Quant. Grav. **15**, L85 (1998); S. Deser and O. Levin, Phys. Rev. D **59**, 064004 (1999).
 - [10] S.W. Hawking, Comm. Math. Phys. **42**, 199 (1975); J.D. Bekenstein, Phys. Rev. D **7**, 2333 (1973); R.M. Wald, *Quantum Field Theory in Curved Spacetime and Black Hole Thermodynamics* (The University of Chicago Press, Chicago 1994); J.D. Brown, J. Creighton and R.B. Mann, Phys. Rev. D **50**, 6394 (1994); R.M. Wald, Living Rev. Rel. **4**, 6 (2001).
 - [11] W.G. Unruh, Phys. Rev. D **14**, 870 (1976); P.C.W. Davies, J. Phys. A **8**, 609 (1975).
 - [12] S.T. Hong, Gen. Rel. Grav. **36**, 1919 (2004).
 - [13] H.Z. Chen, Y. Tian and Y.H. Gao, JHEP **0410**, 011 (2004); H.Z. Chen and Y. Tian, gr-qc/0410077.
 - [14] M. Banados, C. Teitelboim, and J. Zanelli, Phys. Rev. Lett. **69**, 1849 (1992); M. Banados, M. Henneaux, C. Teitelboim, and J. Zanelli, Phys. Rev. D **48**, 1506 (1993).
 - [15] S.T. Hong, Phys. Lett. B **578**, 187 (2004).
 - [16] D.C. Wilkins, Phys. Rev. D **5**, 814 (1972).
 - [17] L.D. Landau and E.M. Lifschitz, *Fluid Mechanics* (Pergamon, Oxford 1977).
 - [18] S.L. Shapiro, Ap. J. **189**, 343 (1974).